Original Article

JNK is critical for the development of *Candida albicans*-induced vascular lesions in a mouse model of Kawasaki Disease

Yukako Yoshikane [a,*], Mitsuhisa Koga [b], Kyoko Imanaka-Yoshida [c,d], Tamaki Cho [e], Yumi Yamamoto [f], Toshimichi Yoshida [c,d], Junichi Hashimoto [a], Shinichi Hirose [a], Koichi Yoshimura [f,g]

[a] Department of Pediatrics, Faculty of Medicine, Fukuoka University, Fukuoka, 814-0180, Japan
[b] Department of Pharmaceutical Care and Health Sciences, Faculty of Pharmaceutical Sciences, Fukuoka University, Fukuoka, 814-0180, Japan
[c] Department of Pathology and Matrix Biology, Mie University Graduate School of Medicine, Tsu, 514-8507, Japan
[d] Mie University Research Center for Matrix Biology, Mie University, Tsu, 514-8507, Japan
[e] Section of Infection Biology, Department of Functional Bioscience, Fukuoka Dental College, Fukuoka, 814-0193, Japan
[f] Department of Surgery and Clinical Science, Yamaguchi University Graduate School of Medicine, Ube, 755-8505, Japan
[g] Graduate School of Health and Welfare, Yamaguchi Prefectural University, Yamaguchi, 753-8502, Japan

ARTICLE INFO

ABSTRACT

Background: Kawasaki disease (KD) is the most common systemic vasculitis of unknown etiology in children, and can cause the life-threatening complication of coronary artery aneurysm. Although a novel treatment strategy for patients with KD-caused vascular lesions is eagerly awaited, their molecular pathogenesis remains largely unknown. c-Jun N-terminal kinase (JNK) is a signaling molecule known to have roles in inflammation and tissue remodeling. The aim of this study was to elucidate significant involvement of JNK in the development of vascular lesions in a mouse model of KD.

Methods and results: We injected *Candida albicans* cell wall extract (CAWE) into 4-week-old C57BL/6 mice. Macroscopically, we found that CAWE caused the development of bulging lesions at coronary artery, carotid artery, celiac artery, iliac artery and abdominal aorta. Histological examination of coronary artery and abdominal aorta in CAWE-treated mice showed marked inflammatory cell infiltration, destruction of elastic lamellae, loss of medial smooth muscle cells and intimal thickening, which are similar to histological features of vascular lesions of patients with KD. To find the role of JNK in lesion formation, we evaluated the effects of JNK inhibitor, SP600125, on abdominal aortic lesions induced by CAWE. Interestingly, treatment with SP600125 significantly decreased the incidence of lesions and also protected against vascular inflammation and tissue destruction histologically, compared with the placebo treatment.

Conclusions: Our findings suggest that JNK is crucial for the development of CAWE-induced vascular lesions in mice, and potentially represents a novel therapeutic target for KD.

1. Introduction

Kawasaki disease (KD), which is the most common systemic vasculitis with unknown origin in childhood, causes inflammation of coronary arteries, leading to development of aneurysms, a life-threatening complication [1–4]. About 25% of children with untreated KD and 5% of those treated with high-dose γ-globulin, the current standard therapy for acute-stage KD [3,5], develop coronary artery aneurysms and remain at risk of myocardial infarction and sudden death until later in life [3,6,7]. Therefore, the need for novel therapeutic targets in KD-caused vascular lesions is critical. However, the pathogenesis of KD is not fully understood.

Some experimental studies of KD that used mouse models have provided potential therapeutic targets for coronary artery vasculitis. In these studies, *Lactobacillus casei* cell wall extract (LCWE) and *Candida albicans* cell wall extract (CAWE) were commonly used to induce a mouse model of coronary arteritis that mimics that of human KD [8–11]. For example, Lee et al. demonstrated the crucial role of interleukin-1β in LCWE-induced coronary arteritis in mice [10]. Martinez et al. reported the role of chemokine receptor-2 in CAWE-induced coronary arteritis in mice [12]. Oharaseki et al. also used CAWE-induced coronary arteritis in mice to examine the role of tumor necrosis factor-α [11]. Although extensive histopathological analyses were conducted to evaluate inflammation in these studies, we needed to

establish a new experimental model system, to enable both macroscopic and histopathologic evaluation of KD-caused vascular lesions.

All aneurysmal lesions, whatever their etiology, share common pathologic hallmarks, including inflammation and proteolytic degradation of the extracellular matrix [13–16]. Excessive matrix proteolysis mediated by matrix metalloproteinases (MMPs), notably MMP-9, is considered a common and critical step during lesion development [13,15,17,18]. In fact, MMP-9 is upregulated in coronary lesions of the LCWE-induced mouse model [19] and also in patients with KD [20]. Inhibition of MMP-9 had been shown to prevent elastin degradation in the LCWE-induced mouse model, but it had no effect on inflammatory infiltration [19], which suggests that upstream signaling molecules would be a desirable target. We then focused on c-Jun N-terminal kinase (JNK), a stress-activated signaling molecule, which regulates MMP-9 and various proinflammatory cytokines [21,22]. SP600125, a specific JNK inhibitor, has been shown to completely block development of abdominal aortic aneurysm in mice, accompanied by reduction of MMP-9 and macrophage infiltration, and preservation of elastic lamellae [23].

We hypothesized that inhibiting JNK would attenuate development of vascular lesions in a mouse model of KD. Initially, we successfully created a mouse model system that allowed us to assess development of the lesions that are compatible with those in KD. Consequently, we showed that pharmacologic inhibition of JNK effectively prevented development of CAWE-induced lesions in mice.

2. Methods

2.1. CAWE preparation

Candida albicans cell wall extract (CAWE) was prepared from *Candida albicans* standard strain SC5314 by modifying the method described previously [9]. Briefly, *Candida albicans* SC5314 stock culture was stored at $-80\ °C$, then incubated at 37 °C for 48 h aerobically on yeast peptone dextrose agar (10 g yeast extract, 20 g peptone, 20 g glucose and 20 g agar per liter). Yeast cells were harvested (about 600 mg wet weight/plate) from agar plates using a scraper and washed three times with distilled water. An extract was obtained by boiling yeast cells for 2 h with 0.5 M KOH (200 mg wet weight of yeast cells/ml). After alkali neutralization in pH7.2 and dialysis against water for 3 days, the extracted material was precipitated with ethanol. The precipitate, about 4% against wet weight yeast cells, was suspended in phosphate-buffered saline (PBS) and adjusted to a final concentration of 100 mg/ml.

2.2. Mice

Four-week-old C57BL/6 N male mice were purchased from Kyudo Co., Ltd. (Tosu, Saga, Japan). Mice were kept in plastic cages (5 per cage) under pathogen-free conditions in a room at $24\pm2.5\ °C$ and $55\%\pm5\%$ relative humidity under a 12:12-h light–dark cycle. Mice were given free access to standard food and water throughout the experiments. All experiments were performed in conformity with the Guide for the Care and Use of Laboratory Animals published by the United States National Institutes of Health. The protocols were approved by the Laboratory Animal Care and Use Committee of Fukuoka University (#116479).

2.3. Induction of vascular lesions in mice

To induce vascular lesions, 4-week-old C57BL/6 male mice were injected intraperitoneally (i.p.) with 4 mg of CAWE for 5 consecutive days every 4 weeks for 2 cycles; and then euthanized with overdoses of sodium pentobarbital (100 mg/kg, i.p.) at 4, 8 or 12 weeks after the second CAWE cycle (Fig. 1A). For whole-body perfusion fixation, 4% paraformaldehyde in PBS was perfused at physiological pressure. After perfusion fixation, the hearts and the whole aortas with branches

were exposed and excised for morphometric and histological analyses. Additionally, in some experiments, a mixture of 10% India ink/4% gelatin in PBS was injected into aortic root to visualize coronary arteries.

2.4. Inhibition of JNK in mice

Custom-made pellets containing JNK-specific inhibitor SP600125 (30 mg/kg/day) and control placebo pellets were purchased from Innovative Research of America (Sarasota, FL, USA). For pellet implantation, 4-week-old C57BL/6 male mice were anesthetized with sodium pentobarbital (40 mg/kg, i.p.). Anesthesia was monitored by periodic observation of respiration and pain response. Pellets were implanted in subcutaneous pockets created on the backs of the mice before starting CAWE administration as described above. The mice were euthanized as described, at 4 weeks after the second CAWE cycle (Fig. 1B). After whole-body perfusion fixation as described, hearts and whole aortas with branches were excised, photographed for morphometric analysis, and analyzed histologically. Photographs of aortas were used to determine maximum external aortic diameters.

2.5. Histological and immunohistochemical analyses

Paraffin-embedded sections were stained with hematoxylin/eosin (HE) and elastica-van Gieson (EVG) for histological analysis. For EVG staining, sirius red was used instead of acid fuchsin. Sections were also probed with antibodies raised against appropriate antigens for immunohistochemistry, as described previously [24]. We detected tenascin-C (TN-C), α-smooth muscle actin (α-SMA), Mac-3 and activated JNK by probing sections with rabbit polyclonal anti-TN-C antibody [25], mouse anti-smooth muscle α-actin antibody (Dako, Glostrup, Denmark), rat anti-Mac-3 antibody (BD Biosciences, San Jose, CA, USA) and rabbit polyclonal anti-phosphorylated JNK (p-JNK) antibody (Promega, Fitchburg, WI, USA), respectively. The sections were visualized with an avidin–biotin–peroxidase complex staining kit (Vector Laboratories, Burlingame, CA, USA) and colorized with diaminobenzidine (DAB) chromogen. For double immunostaining, sections were incubated with anti-p-JNK antibody, visualized with a peroxidase complex staining kit and DAB, and incubated with fluorescein isothiocyanate-conjugated anti-α-SMA (Sigma, St. Louis, MO, USA) or anti-Mac-3 and Alexa Fluor 546 goat anti-rat IgG (Molecular Probes, Eugene, OR, USA). Slides were observed under a fluorescent/differential interference contrast (DIC) microscope (BH2, Olympus, Tokyo Japan). Immunofulorescent signals were superimposed on DIC images.

2.6. Statistical analysis

Data are expressed as mean±standard deviation (SD). Statistical analyses were performed with the Prism 5.0d statistical program (GraphPad Software, La Jolla, CA, USA). We used Fisher's exact test to compare incidence of aneurysm development. We used the Mann Whitney test to compare maximal aortic diameters between experimental groups. A value of $P < 0.05$ was considered statistically significant.

3. Results

3.1. Development of arterial and aortic lesions induced by CAWE

To create a mouse model of KD-related lesions, we injected into 4-week-old C57BL/6 male mice with 4 mg of CAWE for 5 consecutive days for 2 cycles. Four to 12 weeks later, we found that a considerable number of mice developed bulging lesions and that these lesions were created at abdominal aorta, iliac artery, coronary artery, carotid artery, and celiac artery (Fig. 2A-D). Some mice had multiple lesions with a "string of beads" appearance (Fig. 2D). All of the lesions looked pearly white, which indicated that they were
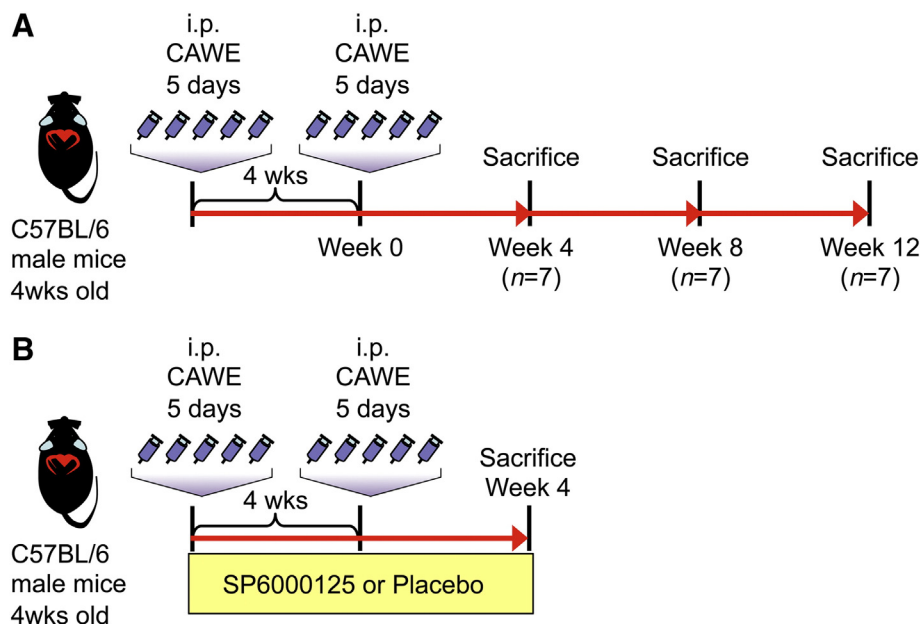
Fig. 1. Experimental design. **A:** To develop a mouse model of Kawasaki disease, *Candida albicans* wall extract (CAWE, 4 mg/body/day) was administered intraperitoneally to 4-week-old C57BL/6 male mice for 5 consecutive days every 4 weeks for 2 cycles. The mice were euthanized at 4, 8 or 12 weeks after the second administration of CAWE. **B:** To examine the role of JNK during development of CAWE-induced lesions, the mice were treated with SP600125 (30 mg/kg/day), pharmacological inhibitor of JNK, or placebo for the entire period of the experiment. The mice were euthanized at 4 weeks after the second administration of CAWE.

accompanied with fibrotic thickening of vessel walls. Most of the lesions were fusiform. These macroscopic observations suggested that these might be aneurysmal lesions. We did not find

Fig. 2. Development of arterial and aortic lesions induced by CAWE. Representative photographs show the arterial and aortic lesions induced by *Candida albicans* wall extract (CAWE) in mice, as indicated by yellow arrows. **A:** Lesion of the left coronary artery (lt CA), which was visualized by India ink perfusion. **B:** Lesion of the right common carotid artery (rt CCA). **C:** Lesion of the pararenal abdominal aorta (AA) at the level of the left renal artery (lt RA). **D:** Lesions of the infrarenal abdominal aorta and the left common iliac artery (lt CIA).

thrombotic occlusion or rupture of aneurysm during the experimental period.

Coronary artery lesions were observed near the orifice of the left main coronary artery only in some CAWE-treated mice (Fig. 3A–C). Coronary arteries of untreated control mice showed preserved elastic lamellae, α-SMA$^+$ medial smooth muscle cells, and few inflammatory cells. In contrast, dilated coronary arteries of CAWE-treated mice showed marked inflammatory cell infiltration into all arterial wall layers, straightening and fragmentation of elastic lamellae, disappearance of α-SMA$^+$ cells in the media, and intimal thickening (Fig. 3B and C). Fibrinoid necrosis was not seen in the experimental mice. These findings are similar to pathological features of KD vascular lesions [26]. We also found TN-C to be greatly expressed, associated with cellular infiltration, medial destruction and intimal hyperplasia in the involved arterial walls of CAWE-treated mice (Fig. 3B and C). TN-C is known to be highly upregulated in the vascular system during inflammatory responses, and its expression could be a marker for active tissue remodeling [24].
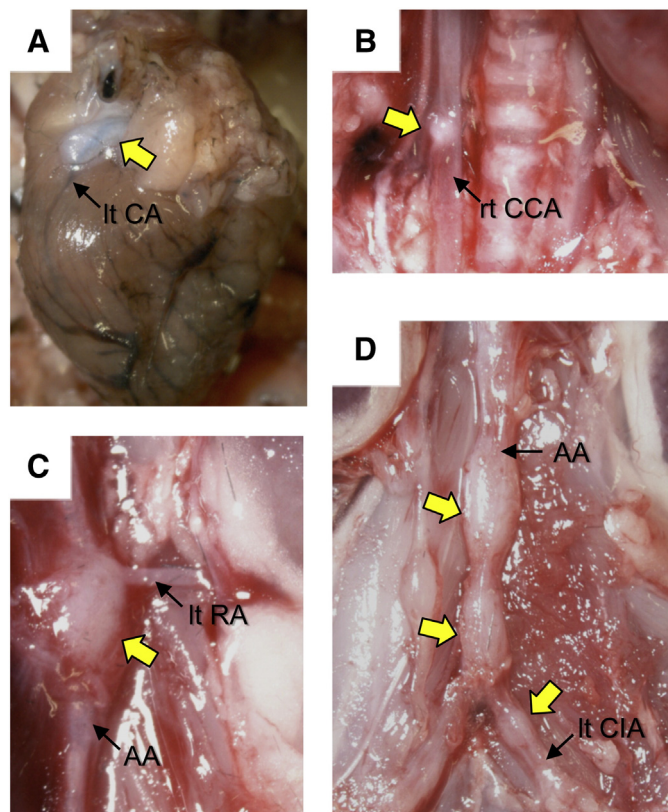
3.2. Temporal pattern of development of CAWE-induced lesions

We next investigated whether the temporal pattern of pathological processes in CAWE-treated artery accords with that in KD. The incidences of coronary artery lesions were 0.0% (0/7 mice), 14.3% (1/7 mice) and 14.3% (1/7 mice) at 4, 8 and 12 weeks, respectively, after CAWE treatment. In the medium-sized vessels, the incidences of arterial lesions (iliac, coronary, carotid and celiac lesions) were 0.0% (0/7 mice), 42.9% (3/7 mice) and 57.1% (4/7 mice) at 4, 8 and 12 weeks, respectively, after the CAWE treatment (Fig. 4A). Thus, the incidences of lesions in medium vessels were modestly high at 8 and 12 weeks after CAWE treatment, but the incidence of coronary artery lesions was not enough for temporal analysis. Fortunately, the incidences of abdominal aortic lesions were 42.9% (3/7 mice), 57.1% (4/7 mice) and 85.7% (6/7 mice) at 4, 8 and 12 weeks, respectively, after CAWE treatment (Fig. 4A). By the definitions adopted by the 2012 International Chapel Hill Consensus Conference on the Nomenclature of Vasculitides (CHCC2012), KD is classified as part of medium vessel vasculitis (MVV). However, as the CHCC2012 definitions also note that aorta and large arteries may be affected [27,28], we used abdominal aortic lesions in the CAWE-treated mice for further studies.
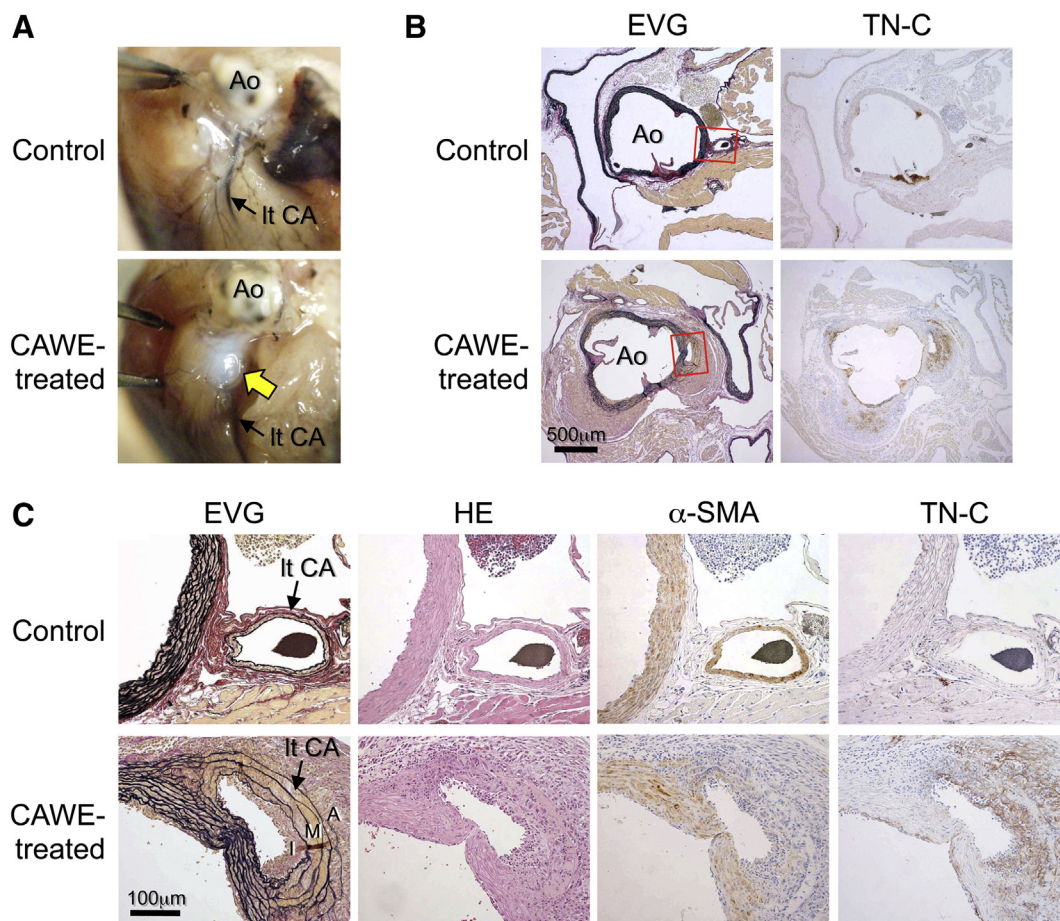
Fig. 3. Development of coronary artery lesions induced by CAWE. **A:** Representative photographs show the left coronary artery (lt CA) originating from the aorta (Ao) in untreated mice (Control) and mice treated with *Candida albicans* wall extract (CAWE-treated). The left coronary artery was visualized by India ink perfusion. Yellow arrows indicate the coronary artery lesion induced by CAWE. **B:** Representative histological and immunohistochemical stains are shown for the aorta (Ao) and the left coronary artery of the control and the CAWE-treated mice. **C:** Representative histological and immunohistochemical stains are shown for enlarged images of the areas within the red squares in the panel B. Elastica van-Gieson (EVG) stain depicts elastin network (black), collagen fibers (red), and muscles (yellow). Hematoxylin/eosin (HE) stain depicts cell nuclei (blue–black). Levels of protein expression and localization of tenascin-C (TN-C) and α-smooth muscle actin (α-SMA) are indicated by brown staining. I: intima, M: media, A: adventitia.

Histological sections of abdominal aortic lesions in CAWE-treated mice also showed similar changes to those of the coronary artery lesions (Fig. 4B and C). At 4 weeks after the CAWE treatment, we observed >marked infiltration of inflammatory cells, including dominant macrophages and lymphocytes, into all layers of the aortic walls. Especially, accumulation of inflammatory cells associated with increased collagen fibers resulted in extensive thickening of the adventitia around the aorta. Although thickness of media and multilayered α-SMA$^+$ smooth muscle cells appeared to be sustained, elastic lamellae began to show straightening and fragmentation. TN-C was widely expressed from intima to adventitia. Inflammatory cell infiltration continued until 8 weeks and gradually decreased at 12 weeks. Destruction of elastic lamellae and thinning of the media progressed until 12 weeks. The α-SMA$^+$ smooth muscle cells completely disappeared in media by 8–12 weeks, whereas neointima consisting of numerous α-SMA$^+$ cells was formed and thickened, leading to stenosis at 12 weeks. TN-C staining was still intense at 8 and 12 weeks, but localized in the thickened intima and the residual media (Fig. 4B and C).

To ascertain if JNK is activated in vascular cells during the development of CAWE-induced lesions, we also examined the tissue localization of p-JNK. Aortic walls of untreated control mice showed few JNK-activated cells. In contrast, dramatic activation of JNK was observed throughout all layers of aortic walls at 4 weeks after CAWE treatment. JNK activation was mostly detected in α-SMA$^+$ smooth muscle cells in the media and the thickened neointima and macrophages were noted in all layers of aortic lesions (Fig. 5A and B).

3.3. Preventive effect of JNK inhibition on development of CAWE-induced lesions

We next investigated whether JNK activation is necessary for development of CAWE-induced lesions. To this end, we subcutaneously implanted the pellets, which were designed to release JNK-specific inhibitor SP600125 (30 mg/kg/day) over the experimental period, in CAWE-treated mice (SP600125 group, n=10). Placebo pellets were also used in CAWE-treated mice as controls (placebo group, n=20). Morphometric analyses of the aortas after perfusion fixation showed that 13 (65.0%) of 20 mice developed abdominal aortic lesions, which reached a certain size and were occasionally accompanied by a "string of beads" appearance, in the placebo group. In contrast, in the SP600125 group, only one (10.0%) of 10 mice developed a small-sized lesion (Fig. 6A and B). Thus, treatment with SP600125 dramatically decreased the incidence of aortic lesions induced by CAWE (P<0.01 compared with the placebo group; Fig. 6B), and also significantly reduced the maximum external diameter of the abdominal aorta (P<0.01 compared with the placebo group; Fig. 6C). Histological analyses showed that development of lesions was accompanied by marked cellular infiltration into all layers of the aortic wall, extensive destruction of the elastic lamellae in the media, and some intimal thickening in the placebo group. Significant macrophage infiltration and TN-C expression were also extended across all layers of the wall. In sharp contrast, most mice in the SP600125 group showed a few inflammatory cells and preserved elastic lamellae (Fig. 6D). These results indicate that treatment
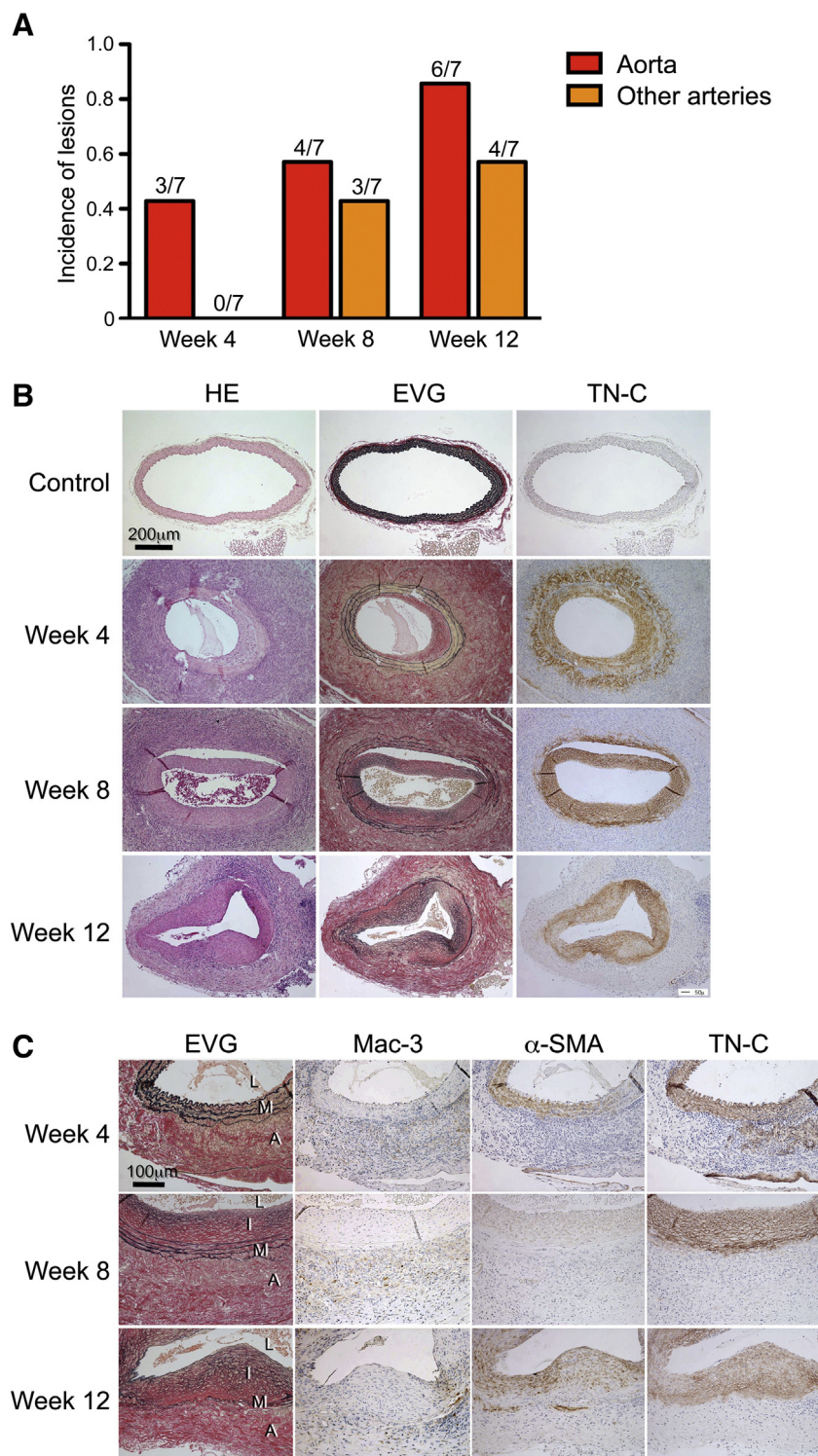
Fig. 4. Development of aortic lesions induced by CAWE. **A**: Mice treated with *Candida albicans* wall extract (CAWE) developed aortic and arterial lesions. Incidences of aortic and other arterial lesions are shown at 4, 8 or 12 weeks after administration of CAWE. **B**: Representative histological and immunohistochemical stains are shown for control aorta from untreated control mice and aortic lesions from the mice sacrificed at 4, 8 or 12 weeks after CAWE treatment. **C**: Representative histological and immunohistochemical stains are shown for enlarged images of aortic lesions from the CAWE-treated mice. Hematoxylin/eosin (HE) stain depicts cell nuclei (blue–black). Elastica van-Gieson (EVG) stain depicts elastin network (black), collagen fibers (red), and muscles (yellow). Levels of protein expression and localization of tenascin-C (TN-C), α-smooth muscle actin (α-SMA) and Mac-3, a macrophage surface glycoprotein, are indicated by brown staining. L: lumen, I: intima, M: media, A: adventitia.

with SP600125 protects against CAWE-induced vascular inflammation and tissue destruction, resulting in suppressed development of lesions. More interestingly, we also observed TN-C to be significantly expressed only in the medial layer, which appeared undamaged, in the SP600125 group. This finding indicates that medial smooth muscle cells were not completely normal in the SP600125 group, and might be under certain pathological conditions (convalescence, e.g.) at least 4 weeks after CAWE treatment.
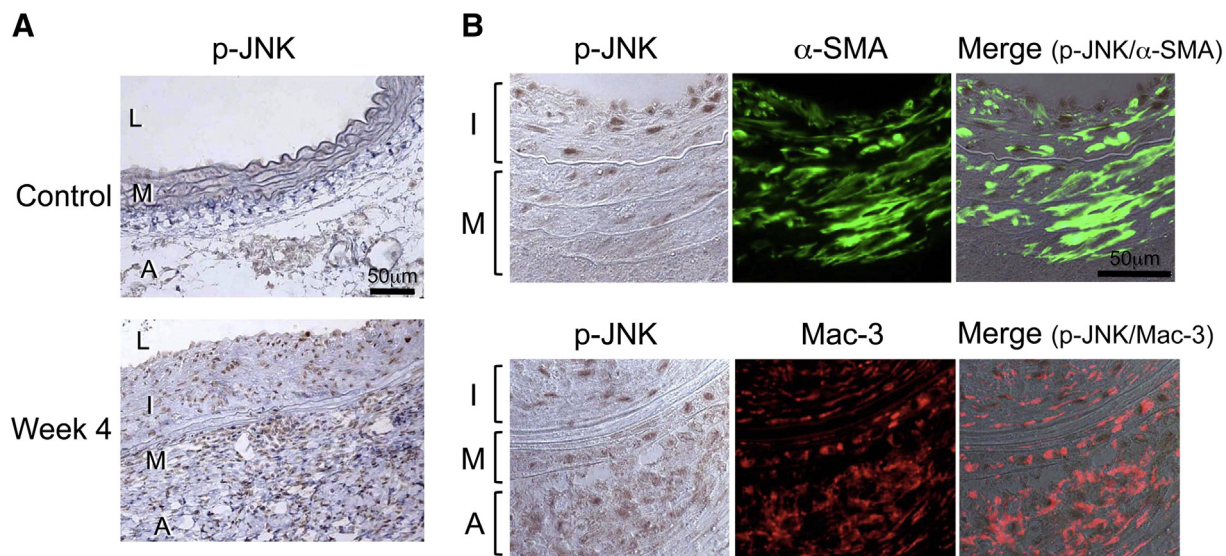
Fig. 5. JNK activation in aortic lesions induced by CAWE. **A:** Representative immunohistochemical stains are shown for control aorta from untreated control mice and aortic lesions from the mice sacrificed at 4 weeks after CAWE treatment. Localization of phosphorylated JNK (p-JNK) is indicated by brown staining. **B:** Representative immunohistochemical and immunofluorescence stains are shown for aortic lesions after CAWE treatment. Activated JNK (p-JNK) is indicated by brown staining in differential interference contrast (DIC) images. Localization of α-smooth muscle actin (α-SMA) positive cells or Mac-3 positive macrophages is indicated by green and red fluorescent signals, respectively. L: lumen, I: intima, M: media, A: adventitia.

4. Discussion

The present study clearly showed that pharmacologic inhibition of JNK significantly prevented the development of CAWE-induced vascular lesions in mice. Prior to this demonstration, we administered CAWE to young mice and created the model system, which substantially imitated KD-caused human artery lesions and allowed us to evaluate both macroscopical and histopathological changes in medium-sized arteries and the aorta. Previous imaging studies in patients with KD have shown that coronary artery aneurysms are commonly fusiform or spherical in shape and occasionally form multiple or complex aneurysms, which may show a "string of beads" appearance [3,29–31]. In this study, these macroscopic characteristics were largely recapitulated in both arterial and aortic lesions of our mouse model. Histological studies of autopsy cases with KD-caused coronary artery aneurysms have shown inflammatory cell infiltration into all arterial wall layers, elastic lamellae destruction and intimal thickening [26,29]. In most settings, the medial layer is very thin, whereas the adventitia is thickened by fibrous proliferation [32]. Additionally, fibrinoid necrosis is a characteristic of polyarteritis nodosa, but not KD [27,33]. Our data clearly showed that these hallmark features of KD pathology were fully recapitulated in our CAWE-induced model.

Pathologic changes over time in KD-caused human coronary arterial lesions have been studied previously. Takahashi et al. reported that inflammatory cells infiltrate arterial walls and lead to panvasculitis approximately 10 days after onset of KD [26]. As inflammation progresses, elastic lamellae and smooth muscle cells become severely damaged, eventually resulting in aneurysm formation. Cellular infiltration persists until about 4 weeks after KD onset, after which the acute inflammatory stage gradually transitions into the convalescent stage. Thereafter, in most patients, coronary arteries tend to develop full circumferential intimal thickening, which can cause thrombotic occlusion [2,26]. These temporal aspects of KD arterial lesions were largely reproduced in our CAWE-induced model.

Obviously, our model and human KD differ in some respects. Particularly the highest incidence of vascular lesion is found in coronary arteries in humans [26,27], whereas incidence of aortic lesions was higher than that of coronary artery lesions in our model. However, the size of children's coronary arteries roughly corresponds to that of mouse aorta rather than mouse coronary artery. Therefore, mouse aorta may mimic human coronary artery in the hemodynamic environment, which potentially affects aneurysm progression [13,34]. In addition, human KD can cause thrombotic occlusion or rupture (a rare complication) in arterial aneurysms [4,26], although neither was observed in this study, probably because of limited period of observation as well as limited number of animals.

KD is linked to various pathogenic agents, including many bacteria and viruses [35]. Many epidemiological findings have pointed out that KD seems like an infectious disease [35,36]. Although the pathogen that triggers human KD has not yet been identified, previous studies, as well as our current study, provide evidence that some bacteria-derived components, such as CAWE and LCWE, can trigger initial systemic inflammation and subsequent local vascular inflammation [8–11,15]. Probably, the systemic inflammation is initiated by recognition of pathogen-associated molecular patterns (PAMPs), which are displayed by CAWE and LCWE; inflammation is then mediated by release of type I interferons and inflammatory cytokines such as tumor necrosis factor (TNF) and interleukin-1 (IL-1) [37,38]. Detection of PAMPs also activates pathogen-specific T and B cells that enhance the inflammatory response, or potentially leads to activation of T and B cells specific for antigens that cross-react with self-antigens [38]. In *Candida albicans* infection or CAWE administration, recognition of *Candida albicans*-associated PAMPs through interaction with pattern recognition receptors (PRRs) such as Toll-like receptors and C-type lectin receptors including dectin-1 and dectin-2, initiates production of cytokines and differentiation of T helper-1 (Th1) and Th17 cells [39–41]. These early immune responses are known to involve activation of mitogen-activated protein kinases, including JNK [37,42]. However, based on our observation that TN-C was obviously expressed even in vessel walls of the SP600125-treated mice, we suspect that pharmacologic inhibition of JNK protects against vascular inflammation and lesion formation rather than against the initial immune responses to CAWE.

The mechanism by which initial systemic immune responses to PAMPs lead to the subsequent vascular inflammation is not well understood. Superantigens derived from bacteria and viruses may be involved in this process [15,43,44]. In addition, molecular mimicry that occurs through cross-reactive recognition between a microbial antigen/MHC and a self-antigen/MHC complex could be also responsible for this onset of vasculitis [38]. In the initiation of vasculitis, as proposed previously, inflammatory cells such as macrophages, neutrophils and T cells are recruited to the vascular walls, and various cytokines/chemokines are released. Coincidentally, endothelial cells and vascular smooth
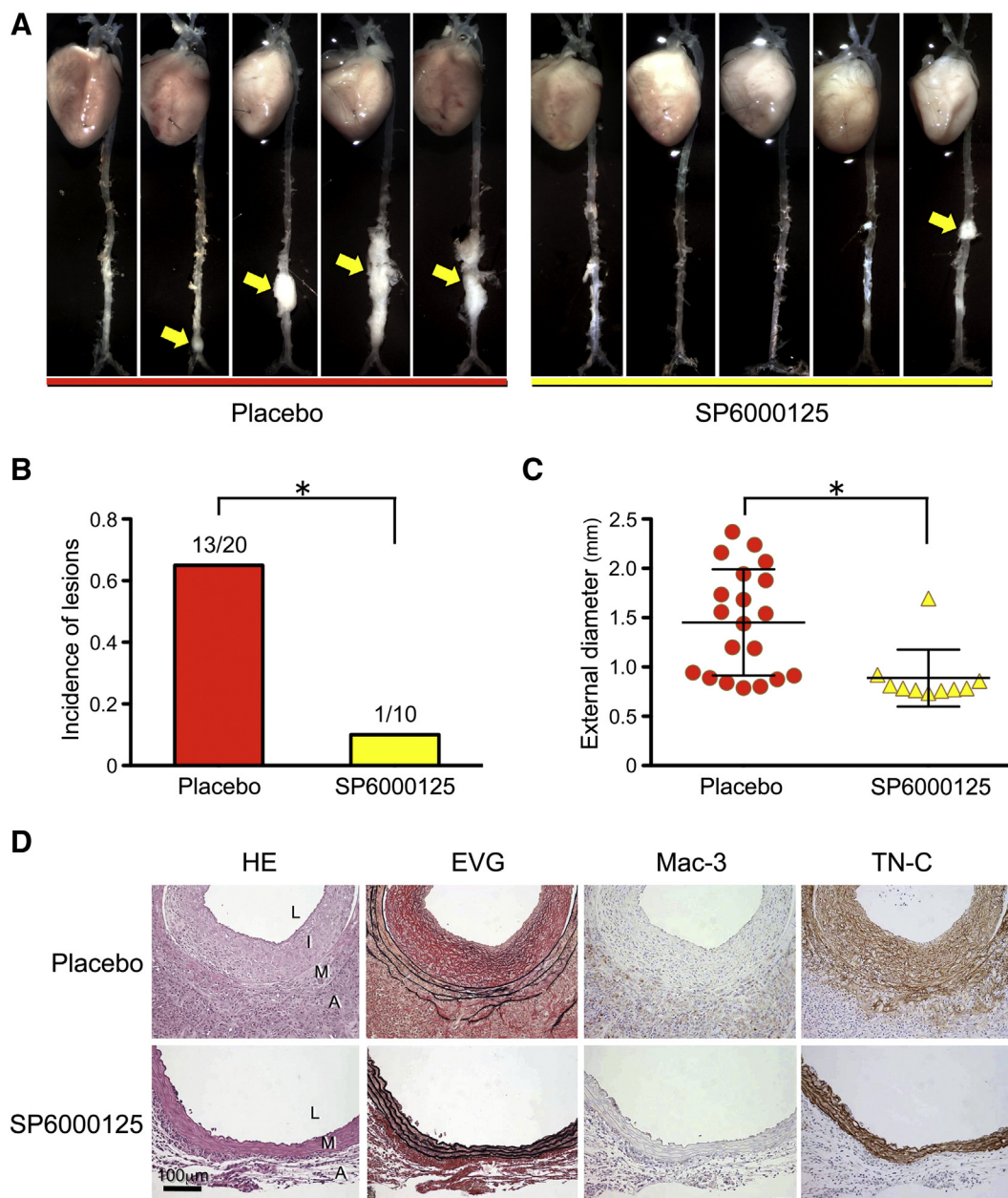
Fig. 6. Effect of JNK inhibition on development of CAWE-induced lesions. **A:** Representative photographs show the aortas of the mice treated with SP600125, JNK inhibitor, or placebo at 4 weeks after administration of *Candida albicans* wall extract (CAWE). **B:** Incidences of aortic lesions induced by CAWE are shown for the mice treated with SP600125 or placebo. **C:** Maximum external diameters of abdominal aortas are shown for the CAWE-treated mice with SP600125 or placebo. Data are mean±SD. * $P<0.01$ compared to placebo. **D:** Representative histological and immunohistochemical stains are shown for the abdominal aortas of the CAWE-treated mice with SP600125 or placebo. Hematoxylin/eosin (HE) stain depicts cell nuclei (blue–black). Elastica van-Gieson (EVG) stain depicts elastin network (black), collagen fibers (red), and muscles (yellow). Levels of protein expression and localization of tenascin-C (TN-C) and Mac-3 are indicated by brown staining. L: lumen, I: intima, M: media, A: adventitia.

muscle cells are also stimulated to produce cytokines/chemokines, which augment inflammatory cell accumulation [15,40]. During these events, JNK can be activated by stimulation with proinflammatory cytokines such as TNF and IL-1 in various cells, including vascular smooth muscle cells and macrophages [23,37]. Activation of JNK also upregulates the genes that encode proinflammatory cytokines such as TNF and IL-1 [21,45,46], thus enhancing these inflammatory responses. A role for JNK in prolongation of vascular inflammation has also been suggested [34,47]. Persistent activation of JNK then contributes to prolonged chronic inflammation and eventually shifts the balance of extracellular matrix metabolism toward degradation by upregulating MMP activity, thereby leading to development of aneurysmal lesions [22,23]. In addition, JNK may also enhance lesion formation by reducing extracellular matrix biosynthetic enzymes including lysyl oxidase [45]

and by mediating apoptosis of vascular smooth muscle cells [48]. Moreover, JNK is reportedly involved in intimal thickening [49], which is typically accompanied by KD-related lesions. Taken together, these data suggest that JNK activation accelerates not only vasculitis but also KD-caused aneurysmal lesions, through multiple mechanisms. We have demonstrated, in fact, that inhibiting JNK suppresses inflammatory cell infiltration, destruction of elastic lamellae and intimal thickening, resulting in effective prevention of lesion formation in our CAWE-induced model.

In conclusion, this study has shown, for the first time, that JNK activation is critical to development of CAWE-induced vascular lesions in mice, and provided novel insights into the role of JNK in the pathogenesis of KD-caused lesion formation. Although further studies are needed to determine the efficacy and safety of JNK inhibition in

KD, our findings suggest that JNK could be a novel therapeutic target in patients with vascular lesions and those at high risk for aneurysms due to nonresponsiveness to current standard therapy.

References

[1] Kawasaki T, Kosaki F, Okawa S, Shigematsu I, Yanagawa H. A new infantile acute febrile mucocutaneous lymph node syndrome (MLNS) prevailing in Japan. Pediatrics 1974;54:271–6.

[2] Burns JC, Glode MP. Kawasaki syndrome. Lancet 2004;364:533–44.

[3] Newburger JW, Takahashi M, Gerber MA, Gewitz MH, Tani LY, Burns JC, et al. Diagnosis, treatment, and long-term management of Kawasaki disease: a statement for health professionals from the Committee on Rheumatic Fever, Endocarditis and Kawasaki Disease, Council on Cardiovascular Disease in the Young, American Heart Association. Circulation 2004;110:2747–71.

[4] Senzaki H. Long-term outcome of Kawasaki disease. Circulation 2008;118:2763–72.

[5] Furusho K, Kamiya T, Nakano H, Kiyosawa N, Shinomiya K, Hayashidera T, et al. High-dose intravenous gammaglobulin for Kawasaki disease. Lancet 1984;2: 1055–8.

[6] Gordon JB, Kahn AM, Burns JC. When children with Kawasaki disease grow up: myocardial and vascular complications in adulthood. J Am Coll Cardiol 2009;54: 1911–20.

[7] Daniels LB, Tjajadi MS, Walford HH, Jimenez-Fernandez S, Trofimenko V, Fick DB, et al. Prevalence of Kawasaki disease in young adults with suspected myocardial ischemia. Circulation 2012;125:2447–53.

[8] Lehman TJ, Walker SM, Mahnovski V, McCurdy D. Coronary arteritis in mice following the systemic injection of group B Lactobacillus casei cell walls in aqueous suspension. Arthritis Rheum 1985;28:652–9.

[9] Takahashi K, Oharaseki T, Wakayama M, Yokouchi Y, Naoe S, Murata H. Histopathological features of murine systemic vasculitis caused by Candida albicans extract—an animal model of Kawasaki disease. Inflamm Res 2004;53:72–7.

[10] Lee Y, Schulte DJ, Shimada K, Chen S, Crother TR, Chiba N, et al. Interleukin-1beta is crucial for the induction of coronary artery inflammation in a mouse model of Kawasaki disease. Circulation 2012;125:1542–50.

[11] Oharaseki T, Yokouchi Y, Yamada H, Mamada H, Muto S, Sadamoto K, et al. The role of TNF-alpha in a murine model of Kawasaki disease arteritis induced with a Candida albicans cell wall polysaccharide. Mod Rheumatol 2013.

[12] Martinez HG, Quinones MP, Jimenez F, Estrada C, Clark KM, Suzuki K, et al. Important role of CCR2 in a murine model of coronary vasculitis. BMC Immunol 2012;13:56.

[13] Tedesco MM, Dalman RL. Arterial aneurysms. In: Cronenwett JL, Johnston KW, editors. Vascular surgery. Philadelphia: Saunders; 2010. p. 117–30.

[14] Yoshimura K, Aoki H. Recent advances in pharmacotherapy development for abdominal aortic aneurysm. Int J Vasc Med 2012;2012:648167.

[15] Yeung RS. Kawasaki disease: update on pathogenesis. Curr Opin Rheumatol 2010; 22:551–60.

[16] Chalouhi N, Hoh BL, Hasan D. Review of cerebral aneurysm formation, growth, and rupture. Stroke 2013;44:3613–22.

[17] Nagasawa A, Yoshimura K, Suzuki R, Mikamo A, Yamashita O, Ikeda Y, et al. Important role of the angiotensin II pathway in producing matrix metalloproteinase-9 in human thoracic aortic aneurysms. J Surg Res 2013.

[18] Aoki T, Kataoka H, Morimoto M, Nozaki K, Hashimoto N. Macrophage-derived matrix metalloproteinase-2 and -9 promote the progression of cerebral aneurysms in rats. Stroke 2007;38:162–9.

[19] Lau AC, Duong TT, Ito S, Yeung RS. Matrix metalloproteinase 9 activity leads to elastin breakdown in an animal model of Kawasaki disease. Arthritis Rheum 2008;58:854–63.

[20] Gavin PJ, Crawford SE, Shulman ST, Garcia FL, Rowley AH. Systemic arterial expression of matrix metalloproteinases 2 and 9 in acute Kawasaki disease. Arterioscler Thromb Vasc Biol 2003;23:576–81.

[21] Zhang YL, Dong C. MAP kinases in immune responses. Cell Mol Immunol 2005;2:20–7.

[22] Yoshimura K, Aoki H, Ikeda Y, Furutani A, Hamano K, Matsuzaki M. Identification of c-Jun N-terminal kinase as a therapeutic target for abdominal aortic aneurysm. Ann N Y Acad Sci 2006;1085:403–6.

[23] Yoshimura K, Aoki H, Ikeda Y, Fujii K, Akiyama N, Furutani A, et al. Regression of abdominal aortic aneurysm by inhibition of c-Jun N-terminal kinase. Nat Med 2005;11:1330–8.

[24] Kimura T, Yoshimura K, Aoki H, Imanaka-Yoshida K, Yoshida T, Ikeda Y, et al. Tenascin-C is expressed in abdominal aortic aneurysm tissue with an active degradation process. Pathol Int 2011;61:559–64.

[25] Imanaka-Yoshida K, Hiroe M, Nishikawa T, Ishiyama S, Shimojo T, Ohta Y, et al. Tenascin-C modulates adhesion of cardiomyocytes to extracellular matrix during tissue remodeling after myocardial infarction. Lab Invest 2001;81:1015–24.

[26] Takahashi K, Oharaseki T, Yokouchi Y, Naoe S, Saji T. Kawasaki disease: basic and pathological findings. Clin Exp Nephrol 2013;17:690–3.

[27] Jennette JC, Falk RJ, Bacon PA, Basu N, Cid MC, Ferrario F, et al. 2012 revised International Chapel Hill Consensus Conference nomenclature of vasculitides. Arthritis Rheum 2013;65:1–11.

[28] Jennette JC. Overview of the 2012 revised International Chapel Hill Consensus Conference nomenclature of vasculitides. Clin Exp Nephrol 2013;17:603–6.

[29] Naoe S, Takahashi K, Masuda H, Tanaka N. Kawasaki disease. With particular emphasis on arterial lesions. Acta Pathol Jpn 1991;41:785–97.

[30] Goo HW, Park IS, Ko JK, Kim YH. Coronary CT angiography and MR angiography of Kawasaki disease. Pediatr Radiol 2006;36:697–705.

[31] Baker AL, Newburger JW. Cardiology patient pages. Kawasaki disease. Circulation 2008;118:e110–2.

[32] Suzuki A, Miyagawa-Tomita S, Komatsu K, Nishikawa T, Sakomura Y, Horie T, et al. Active remodeling of the coronary arterial lesions in the late phase of Kawasaki disease: immunohistochemical study. Circulation 2000;101: 2935–41.

[33] Takahashi K, Oharaseki T, Yokouchi Y. Pathogenesis of Kawasaki disease. Clin Exp Immunol 2011;164(Suppl 1):20–2.

[34] Yamashita O, Yoshimura K, Nagasawa A, Ueda K, Morikage N, Ikeda Y, et al. Periostin links mechanical strain to inflammation in abdominal aortic aneurysm. PLoS One 2013;8:e79753.

[35] Principi N, Rigante D, Esposito S. The role of infection in Kawasaki syndrome. J Infect 2013;67:1–10.

[36] Frazer J. Infectious disease: blowing in the wind. Nature 2012;484:21–3.

[37] Gaestel M, Kotlyarov A, Kracht M. Targeting innate immunity protein kinase signalling in inflammation. Nat Rev Drug Discov 2009;8:480–99.

[38] Munz C, Lunemann JD, Getts MT, Miller SD. Antiviral immune responses: triggers of or triggered by autoimmunity? Nat Rev Immunol 2009;9:246–58.

[39] Cassone A. Development of vaccines for Candida albicans: fighting a skilled transformer. Nat Rev Microbiol 2013;11:884–91.

[40] Takahashi K, Oharaseki T, Yokouchi Y. Update on etio and immunopathogenesis of Kawasaki disease. Curr Opin Rheumatol 2014;26:31–6.

[41] Lin IC, Suen JL, Huang SK, Huang SC, Huang HC, Kuo HC, et al. Dectin-1/Syk signaling is involved in Lactobacillus casei cell wall extract-induced mouse model of Kawasaki disease. Immunobiology 2013;218:201–12.

[42] Arthur JS, Ley SC. Mitogen-activated protein kinases in innate immunity. Nat Rev Immunol 2013;13:679–92.

[43] Devore-Carter D, Kar S, Vellucci V, Bhattacherjee V, Domanski P, Hostetter MK. Superantigen-like effects of a Candida albicans polypeptide. J Infect Dis 2008;197: 981–9.

[44] Duong TT, Silverman ED, Bissessar MV, Yeung RS. Superantigenic activity is responsible for induction of coronary arteritis in mice: an animal model of Kawasaki disease. Int Immunol 2003;15:79–89.

[45] Yoshimura K, Aoki H, Ikeda Y, Furutani A, Hamano K, Matsuzaki M. Regression of abdominal aortic aneurysm by inhibition of c-Jun N-terminal kinase in mice. Ann N Y Acad Sci 2006;1085:74–81.

[46] Guma M, Firestein GS. c-Jun N-terminal kinase in inflammation and rheumatic diseases. Open Rheumatol J 2012;6:220–31.

[47] Onoda M, Yoshimura K, Aoki H, Ikeda Y, Morikage N, Furutani A, et al. Lysyl oxidase resolves inflammation by reducing monocyte chemoattractant protein-1 in abdominal aortic aneurysm. Atherosclerosis 2010;208:366–9.

[48] Takagi Y, Ishikawa M, Nozaki K, Yoshimura S, Hashimoto N. Increased expression of phosphorylated c-Jun amino-terminal kinase and phosphorylated c-Jun in human cerebral aneurysms: role of the c-Jun amino-terminal kinase/c-Jun pathway in apoptosis of vascular walls. Neurosurgery 2002;51: 997–1002 [discussion—4].

[49] Izumi Y, Kim S, Namba M, Yasumoto H, Miyazaki H, Hoshiga M, et al. Gene transfer of dominant-negative mutants of extracellular signal-regulated kinase and c-Jun NH2-terminal kinase prevents neointimal formation in balloon-injured rat artery. Circ Res 2001;88:1120–6.